

SEPTEMBER 1981

LRP 193/81

ON THE NUMERICAL DETERMINATION OF IDEAL MHD LIMITS
OF STABILITY OF AXISYMMETRIC TOROIDAL CONFIGURATIONS

R. Gruber, Ch. Pfersisch, S. Semenzato,
F. Troyon, T. Tsunematsu

prepared for presentation at

the European Workshop on "Computational MHD Models
of the Behaviour of Magnetically-Confined Plasmas"
at Wildhaus-Switzerland, September 1981.

On the numerical determination of ideal MHD limits of stability of
axisymmetric toroidal configurations.

R. Gruber, Ch. Pfersisch, S. Semenzato, F. Troyon, T. Tsunematsu*

EURATOM-Switzerland Fusion Association,
Centre de Recherche en Physique des Plasmas,
Ecole Polytechnique Fédérale de Lausanne,
CH-1007 Lausanne, Switzerland

*Present address: Japan Atomic Energy Research Institute,
Tokai-Mura, Naka-Gun, Japan

ABSTRACT

The various problems that are encountered in searching with ERATO the limits of stability of axisymmetric toroidal equilibria are described and illustrated with specific examples.

1. INTRODUCTION

The value of any computer code, no matter how well it has been tested, can only be assessed after it has been utilized in a number of different situations. MHD spectral codes have been in operation for some years, mainly to study β limits in specific axisymmetric configurations. In this paper we describe our own experience with one of these codes, ERATO [1], the problems and the difficulties in interpretation encountered and how we have solved them. We hope this information will be useful to all ERATO users and especially to the newcomers in the field.

2. THE EIGENVALUE PROBLEM

The eigenmodes of an axisymmetric toroidal plasma, corresponding to a given toroidal wave number n , can be obtained by extremizing the Rayleigh quotient

$$\omega^2 = \frac{\delta W_p[\xi, \xi] + \delta W_v[\xi', \xi']}{\delta W_k[\xi, \xi]} \quad (1)$$

where δW_p , δW_v are the changes in the plasma potential energy and the vacuum energy caused by a displacement $\xi(r)$ of the plasma equilibrium and δW_k is the norm of ξ weighted with the plasma density. The complex displacement vector ξ , which is also the eigenvector of the resulting eigenvalue problem, is a function of 2 variables defined in a poloidal plane : a radial variable $s \equiv \sqrt{\psi/\psi_i}$, where ψ is the usual poloidal flux function, which varies between 0 (magnetic axis) and 1(plasma surface), and an azimuthal angle χ ,

chosen to vary between $-\pi$ and π as shown in Fig. 1. The index i designates the plasma surface. The expressions of the various terms of Eq. (1) in terms of $\xi(s, r)$ one given in Ref.[1].

Substituting the resulting eigenvector $\underline{\xi}$ into Eq. (1), the Rayleigh quotient becomes equal to the eigenvalue ω^2 . The physical displacement $\underline{\xi}_{ph}$ is obtained from the complex eigenvector $\underline{\xi}$ through

$$\underline{\xi}_{ph} = \text{Re} \left[\underline{\xi}(s, r) e^{in\phi} \right] \begin{cases} \cos \omega t & \text{if } \omega^2 > 0 \\ e^{|\omega|t} & \text{if } \omega^2 < 0, \end{cases} \quad (2)$$

where ϕ is the toroidal angle around the main axis.

Stability depends only on the sign of the lowest eigenvalue ω_{\min}^2 . In most cases of interest, singular surfaces defined by $nq = m$, where q is the local safety factor, n the toroidal wave number and m an integer, lie within the plasma. This implies the existence of overlapping stable Alfvén continuums reaching the marginal point $\omega^2 = 0$. The pressure of the plasma vanishes at the surface so that the slow wave continuum extends also to the marginal point. The continuum extends all the way to $\omega^2 = +\infty$ because of the toricity and non-circularity of flux surfaces. Discrete modes can only exist in the unstable region $\omega^2 < 0$. If the Mercier criterion is violated on any singular surface there is an infinite number of unstable eigenmodes, the eigenvalues of which accumulate to the marginal point. If the Mercier criterion is satisfied on all singular surfaces there is a finite number of unstable modes. The limit of stability corresponds to the moment when the last unstable mode reaches the highly degenerate end-point of the continuum at $\omega^2 = 0$. If the lowest eigenvalue ω_{\min}^2

is plotted against a characteristic parameter, such as the plasma β , the resulting $\omega^2_{\min}(\beta)$ is expected to reach the marginal point $\omega^2 = 0$ from the unstable side with a non-vanishing slope $d\omega^2_{\min}/d\beta$. The break in the slope of $\omega^2_{\min}(\beta)$ corresponds to the limit of stability.

3. DISCRETIZATION EFFECTS ON THE SPECTRUM

For the numerical treatment, half the plasma domain, $0 < s < 1$, $0 < \chi < \pi$, is divided into N_s intervals in s and N_χ in the direction χ . The equilibrium is assumed to have up-down symmetry with respect to the mid-plane. In ERATO, the displacement vector $\underline{\xi}(s, \chi)$ is expanded in hybrid finite elements of lowest order. The spectrum is discrete, the continuum being represented by a dense discrete spectrum. The transition between the true discrete modes and those that will eventually become part of the continuum is no longer clear (Fig. 2). Weakly growing modes have a structure reminiscent of a true singular mode, with a large shear displacement on the singular surfaces. The denominator in Eq (1) receives a large contribution from the vicinity of the singular surfaces, which explains the low growthrate. In order to identify correctly the mode it is necessary to do a convergence study which requires calculating ω^2 for a number of values of N_s , N_χ and extrapolating to $N = \infty$.

4. GENERAL CONVERGENCE PROPERTIES

We are only interested in the lowest eigenvalue which determine if the plasma is stable or not. If the plasma is stable this eigenvalue will converge to $\omega^2 = 0$, the marginal point. It is

unstable it will converge to some $\omega^2 < 0$. It cannot converge to a positive value. This is a point which has been missed in the past. When the curve $\omega^2_{\min}(N)$ seems to converge to $\omega^2 > 0$ it is a sure sign that resolution is not sufficient. It happened frequently with the early versions of ERATO when the highest feasible resolution was of the order of $N_S = N_{\text{max}} = 30$ and it will still happen when one tries to calculate high values of n .

The discretization error on δW_p and δW_k is quadratic in the mesh size ($O(N^{-2})$). In the standard version of ERATO the vacuum contribution is evaluated by solving a Fredholm equation with a singular kernel. Because of the way in which the singular term has been handled the discretization error of the off-diagonal terms is expected to be asymptotically in $O(N^{-2} \ln N)$. But $\ln N$ is a slowly varying function of N and the discretization error of the diagonal term has no $\ln N$ term, so that the error may look more like $O(N^{-2})$ when the range of N is not sufficiently large. This mixed behaviour has indeed been a source of uncertainty when the eigenmode shows a sizeable surface motion. In the new vacuum treatment introduced recently as an option for the case where there is a shell which limits the extension of the vacuum region, the discretization error is the same as in the plasma, namely quadratic in the mesh size.

These asymptotic convergence laws are in fact upper bounds on the error due to discretization. The coefficients cannot be evaluated. The real error $\omega^2_N - \omega^2_\infty$ is not a smooth function of N . It can become very noisy in the vicinity of the marginal point.

The error is a rapidly increasing function of the wavenumber n . All unstable modes have a fast dependence given by the ballooning mode theory,

$$\epsilon = \epsilon e^{inqr} \quad (3)$$

To follow this oscillation, the number of intervals N_r has to increase as n . The number of singular surfaces increases too as n , so that N_s has also to increase as n , or maybe \sqrt{n} if the mesh is properly adjusted to match the radial localisation of the mode. The computing time then increases at least as $n^{7/2}$ just to keep the same accuracy. The quasi-mode option described in Reference [2] has been introduced precisely to solve this problem.

In these considerations it is assumed that equilibrium quantities are known. In practice, the flux function $\psi(r,z)$ is obtained numerically by solving the Grad-Shafranov equation discretized on a rectangular mesh. All the equilibrium quantities needed for ERATO are obtained from this table of values of ψ by interpolation, fitting and differencing. The error associated with this procedure is not included. It is certainly a source of noise in the equilibrium quantities. Since we do not know how it affects the convergence laws of ERATO, it is necessary to calculate the equilibrium with as high a resolution as possible to make it more accurate than ERATO at the highest values of N . A better solution is not yet available.

We have gathered during the last few years a large amount of information on how to use effectively ERATO to determine limits of stability. Both Tokamaks and Spheromaks have been studied. We present the most "typical" problems that have been encountered. By typical we mean problems that are always met but never mentioned.

5. THE TOKAMAK REGIME

The Tokamak regime is characterized by the fact that $dq/ds > 0$ everywhere. There are always unstable modes, at any resolution, which means that the discretization scheme is pessimistic. A stable plasma will only be found stable in the limit $N \rightarrow \infty$. The main advantage is that by converging the most unstable mode one obtains a good estimate of the accuracy of the final result, with an upper bound on the growthrate of the most unstable mode. It is not possible to miss an instability. As an illustration we use the results obtained in a study on β limits in INTOR [3]. A sequence of equilibria having the INTOR D-shape (aspect ratio = 4, elongation = 1.6) has been generated by solving the Grad-Shafranov equation with the source terms.

$$\begin{aligned} \frac{d\rho}{d\psi} &= -\alpha_1 \tilde{\psi} - \alpha_2 \tilde{\psi}^2, \\ T \frac{dT}{d\psi} &= \alpha_3 R_m^2 \tilde{\psi}, \end{aligned} \quad \tilde{\psi} \equiv \psi - \psi_c', \quad (4)$$

R_m is the radius of the magnetic axis. The constants α_2 and α_3 are adjusted to keep $q_0 \sim 1.15$ and $q_I = 2.4$ constant, while α_1 is changed. Instead of α_1 it is more convenient to use the plasma β (volume average). We determine with the standard ERATO the growthrate of the most unstable $n = 1$ mode, assuming an infinite vacuum around the plasma and a flat density profile. Fig. 3 shows the square of the growthrate, normalized to the Alfvén transit frequency across the main radius R_m , using a linear scale and a logarithmic scale. The resolution is held constant with $N_S = 2N \chi = 60$. On the linear scale there is a change of slope which one might be tempted to ignore by extrapolating linearly to the marginal point. This might appear justified by the change of character of the mode, which develops an

internal structure with large shear flow around the 2 singular surfaces $q = 2$ and $q = 3$ in the plasma. This was standard practice until very recently. But looking at the logarithmic scale nothing striking occurs until $\omega_{\min}^2 \sim 10^{-4} \omega_A^2$ where there is a pedestal.

A convergence study is clearly needed to identify the correct limit of stability. In the range $|\omega_{\min}^2| > 10^{-3} \omega_A^2$ a plot of ω_{\min}^2 versus N^{-2} , keeping $N_S = 2N_{\chi}$, gives a smooth curve and the extrapolated value shows little difference from the 60/30 value. But at lower $|\omega_{\min}^2|$, the convergence curves, $\omega_{\min}^2(N)$, become progressively noisy and the modes peak more and more on the singular surfaces. Fig. 4 shows such a convergence for one the equilibrium of the series, at $\beta = 2.2\%$. The points obtained with an equidistant mesh do not fit smoothly on a straight line. By concentrating points around the singular surfaces the convergence is improved, although there remains some noise. If the two points at $N_S = 70$ and 90 , which corresponds to odd values of N_{χ} are eliminated the convergence is quadratic and extrapolation shows a residual unstable mode with very small growthrate. It is an empirical fact that one should use in a convergence study values of N_S, N_{χ} with fixed parities. We have not verified in this case if the residual instability is due to inaccuracies of the equilibrium, since such a small growthrate and such a highly singular mode are not physically relevant. In the Rayleigh quotient given by Eq. (1) there is a cancelation in the numerator which becomes more complete as N increases, and the denominator becomes larger as the eigenvector peaks on the singular surfaces. The noise on the convergence curve is sensitive to the radial distribution of the points around the singular surfaces. By

working systematically with a concentrated radial mesh the pedestal at 10^{-4} drops sharply. These results are an indication that the pedestal at 10^{-4} will converge at the marginal point. In this INTOR study we have concluded that the stability limit corresponded to $\omega_{\min}^2 / \omega_A^2 = 10^{-4}$ for a resolution of 60/30, doing occasional convergence studies to verify that the eigenvalue drops rapidly as the resolution is increased.

Our second example shows the problem encountered with larger values of n and how it has been solved. The equilibrium is a well documented high β JET equilibrium proposed in Ref. [4], with a shell tight against the plasma surface so that there are only internal modes. The current is chosen such that ballooning modes are unstable. With the standard version of ERATO one finds it is indeed unstable for all n . But these modes have to be converged. The convergence curves are shown in Fig. 5 for $n = 1, 3$ and 5 (dotted lines). In this study $N_S = N_{\pi}$. The extrapolation is not credible for $n \gtrsim 3$. On the same figure the convergence curves obtained with the new quasi-mode option are shown (solid lines) for the same values of n , and to demonstrate its power, at higher values of n . Quadratic convergence is clean in all cases. We have also used it on the same INTOR equilibria used in Fig. 4 with $n = 2$ and the shell tight on the plasma. We find clean quadratic convergence to the marginal point $\omega^2 = 0$. We have not had enough experience to claim that the quasi-mode version with the new treatment of the vacuum has no difficulties, but we have not yet found any, while it has already solved the problem of calculating intermediate values of n .

6. SPHEROMAK REGIME

The spheromak regime is characterized by $dq/ds < 0$ and $q = 0$ at the plasma surface. It is probable that ERATO will behave the same way in any configuration with $dq/ds < 0$ (including screw-pinches and reversed field configurations), but we do not have enough experience to back such a claim. We have made extensive calculations on the limits of stability of Spheromaks and we use these as evidence that the convergence properties are different in this regime from that in the Tokamak regime. The sequence of Spheromak equilibria is generated by solving the Grad-Shafranov equation with the source terms

$$\frac{dp}{d\psi} = \alpha_1 \psi, \quad T \frac{dT}{d\psi} = \alpha_2 (\psi - \psi_i), \quad (5)$$

and fixing α_2 such that $T(\psi_i) = 0$ when $\alpha_1 = 0$. The plasma has an elongated D shape with an aspect ratio of 1.45. The q profile is insensitive to the pressure in a large range of β (α_1). The maximum value of q is at the magnetic axis and is about .67. The main difference with the Tokamak regime is that, at low resolution and with a shell tight on the plasma (internal modes only), all eigenvalues are on the stable side $\omega^2 > 0$. The first mode is very near $\omega^2 = 0$. To obtain any unstable mode it is necessary to increase the resolution.

The advantage is that once the unstable mode becomes visible the eigenvalue converges nicely. The main inconvenience is that when no unstable mode is found one is never sure that an unstable mode will not appear at higher resolution. Fig. 6 is an example we have encountered. There $|\omega_{\min}^2| / \omega_A^2$ for $n = 2$ is plotted versus β

(α_1). At high β , the values are converged, but the curve stops suddenly when no unstable mode is found at the highest resolution we can use on our computer. Extrapolation to $\omega_{\min}^2 = 0$ would give a critical β of the order of 8 %. But we know that the Mercier criterion is violated on the $q = 0.5$ singular surface at $\beta > \beta_C \approx 3\%$ so that there should be an infinite number of unstable modes in this range. Fig. 7 shows at least part of the problem. The strong radial localization of the mode requires a large number of radial intervals to be correctly represented. The distribution of the potential energy density averaged over a magnetic surface is represented in Fig. 8. There is a cancellation between the positive and negative contributions which becomes more complete as β decreases. When the width of the unstable region, Δs , is plotted versus β (Fig. 9) extrapolation to zero-width gives the same value of β as the Mercier limit on $q = 0.5$.

An interesting comparison can be made with the Tokamak regime. In the Tokamak case the discretized expression for the plasma potential energy corresponding to the lowest eigenvalue, does not change sign as resolution is increased. So the marginal point can only be reached in the limit $N \rightarrow \infty$. In the case of the Spheromak the sign can change as resolution is increased. Since extrapolation from the stable side is impossible the computation of the internal modes stability of Spheromaks is very costly. With a vacuum region the convergence behaviour is very similar to that of Tokamaks.

CONCLUSION

We have shown that ERATO is a powerful tool to study limits of stability of Tokamak configurations. Working first at low resolution the most unstable mode can be found and diagnosed (mode, potential energy, distribution). Selected convergence studies are usually sufficient to identify the critical growthrate below which it can be assumed that it will converge to the marginal point. The standard version of ERATO cannot be used for n large. The new version of ERATO, with its quasi-mode representation and its new vacuum solution, extends considerably the range of n . In Spheromak configurations it appears that, except for the fastest growing free boundary modes, high resolution is needed to find the correct limit of stability.

REFERENCES

- [1] R. Gruber, F. Troyon, D. Berger, L.C. Bernard, S. Rousset, R. Schreiber, W. Kerner, W. Schneider, K.V. Roberts, Comp. Phys. Commun. 21 (1981), 323
- [2] F. Troyon, T. Tsunematsu, W. Kerner, P. Merkel, W. Schneider, in this same issue.
- [3] International Tokamak Reactor (INTOR), IAEA, Vienna, 1980
- [4] A. Sykes, I.A. Wesson, S.J. Cox, Phys. Rev. Letters, 39 (1977), 751 and R. Gruber, R. Schreiber, F. Troyon, W. Kerner, K. Lackner, A. Sykes, J. Wesson
- [5] P. Gauthier, R. Gruber, F. Troyon, Lausanne Report LRP 176/80, Ideal MHD Stability of Oblate Spheromaks, submitted to Nuclear Fusion.

FIGURE CAPTIONS

Fig. 1 The s, χ coordinate system

Fig. 2 Comparison between the exact and discretized spectra

Fig. 3 The lowest $n = 1$ eigenvalue $|\omega_{\min}^2|/\omega_A^2$ as a function of the plasma β . The parameters of this sequence of equilibria are those contemplated for INTOR. In a the scale is linear while it is logarithmic in b.

Fig. 4 Convergence plot of $|\omega_{\min}^2|/\omega_A^2$ as a function of the number of radial intervals N_S , keeping $N_\chi = N_S/2$, using 2 different radial mesh concentrations.

Fig. 5 Convergence plot of $\omega_{\min}^2/\omega_A^2$ as a function of the number of intervals $N = N_S = N_\chi$ for some selected values of n . The dotted curve is obtained with the standard ERATO while the solid curves are obtained with the quasi-mode representation.

Fig. 6 The lowest $n = 2$ eigenvalue Γ^2/ω_A^2 as a function of the plasma β , for a Spheromak surrounded by a rigid boundary at the surface.

Fig. 7 Localization of the internal $n = 2$ unstable mode around the singular surface $q = 0.5$ as a function of β .

Figure Captions (cont'd)

Fig. 8 The radial profile of the plasma potential energy density, averaged over each magnetic surface, showing the localization of the unstable region.

Fig. 9 The width of the unstable region Δ as a function of the plasma β .

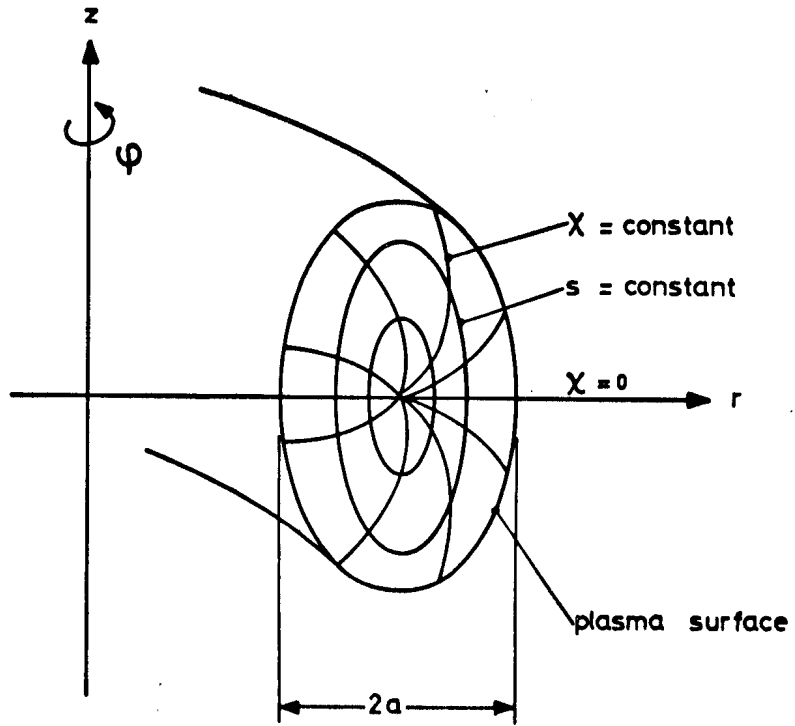


Fig. 1

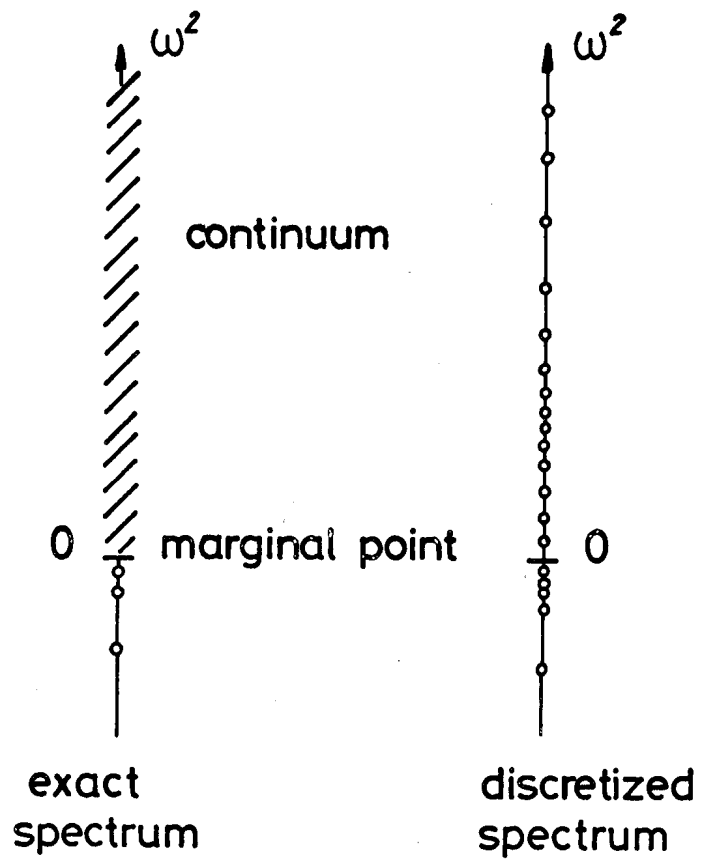


Fig. 2

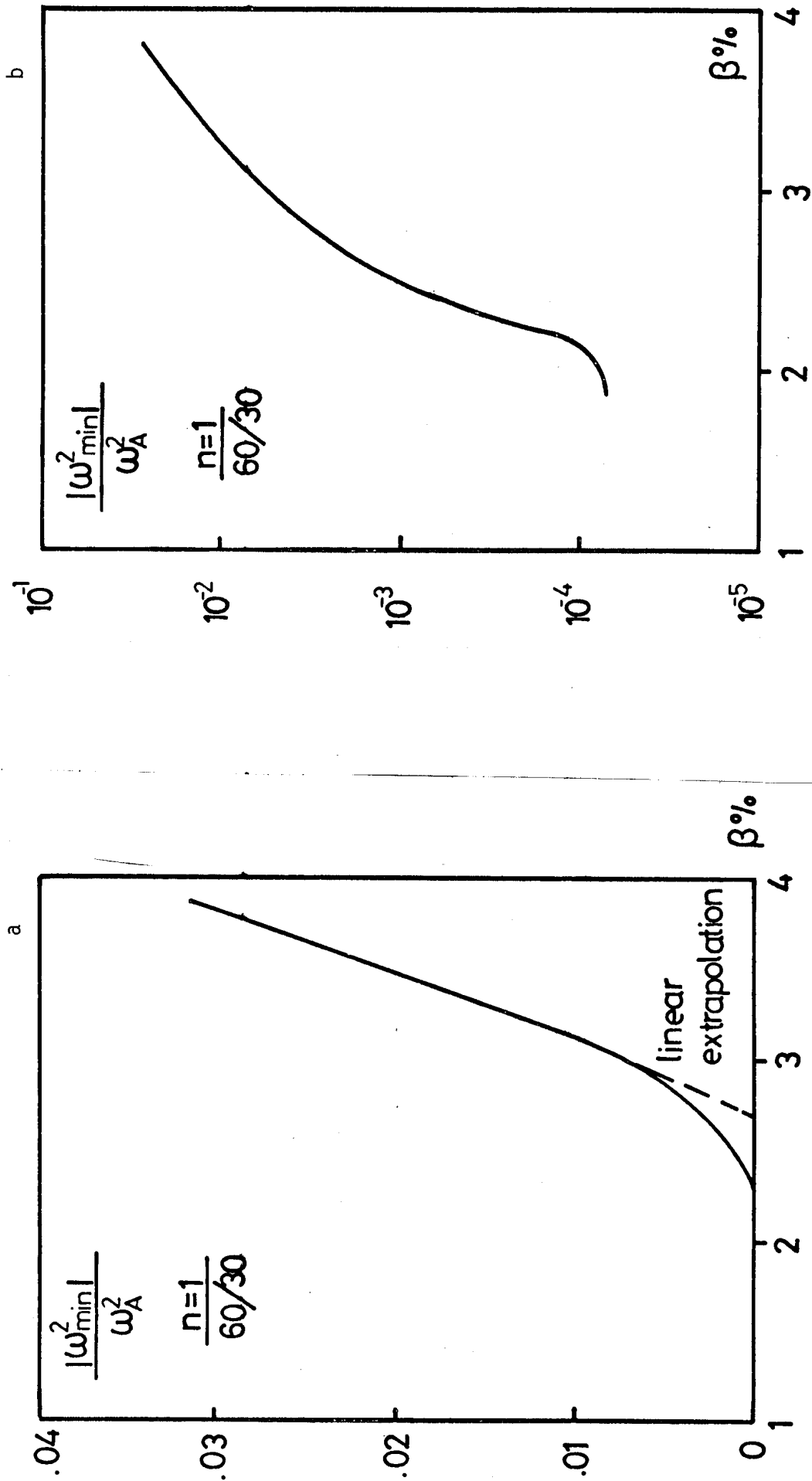


Fig. 3

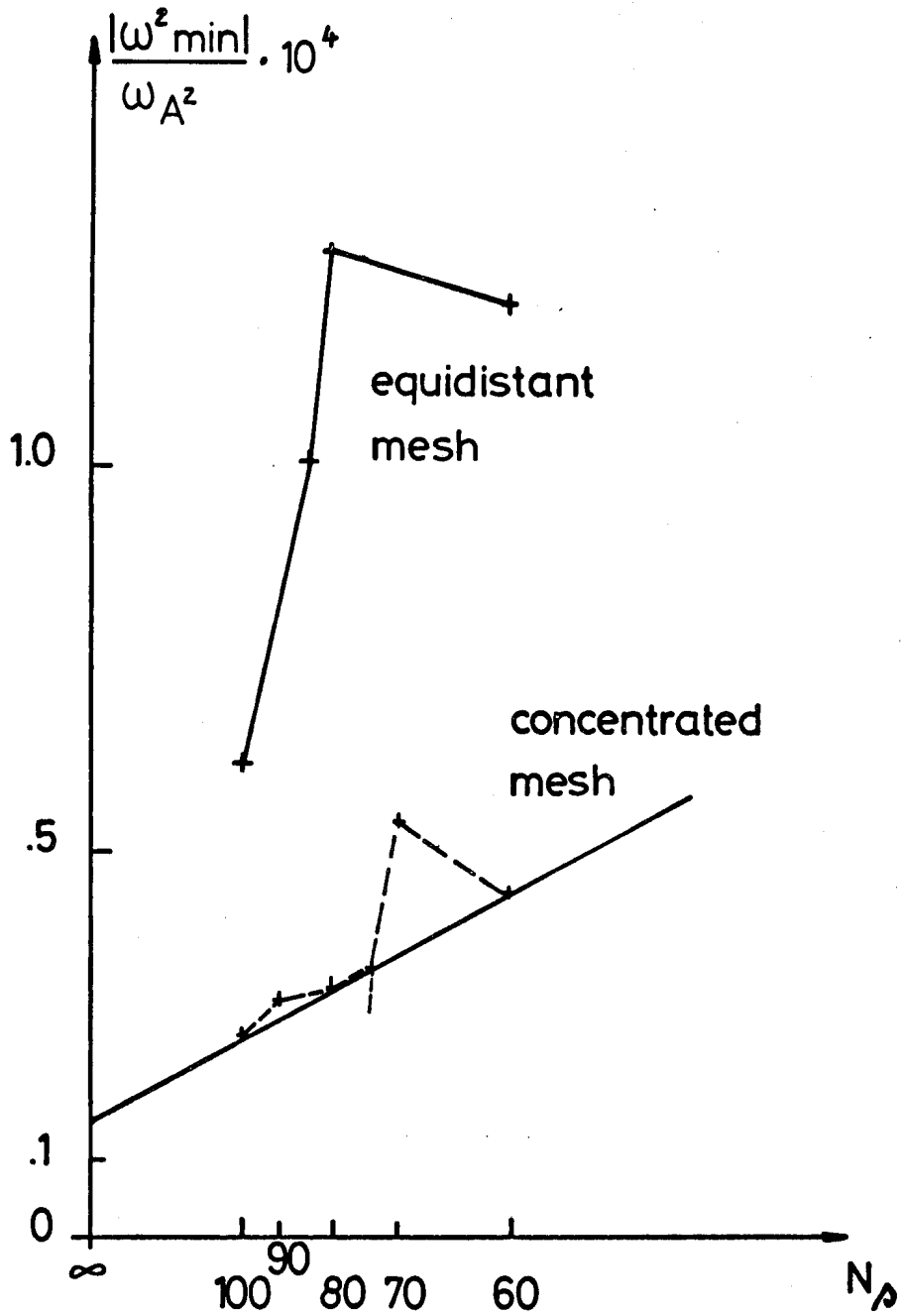


Fig. 4

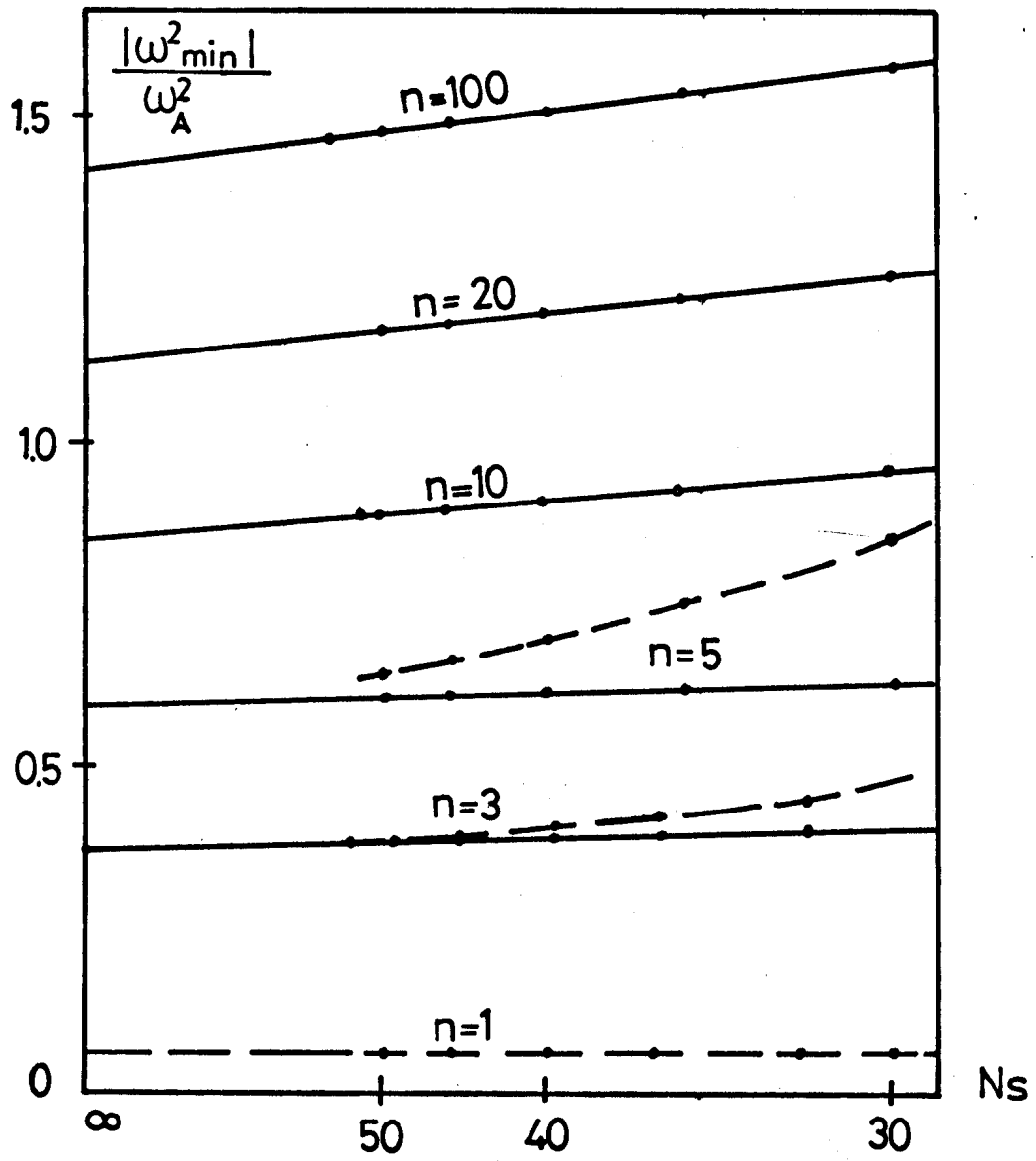


Fig. 5

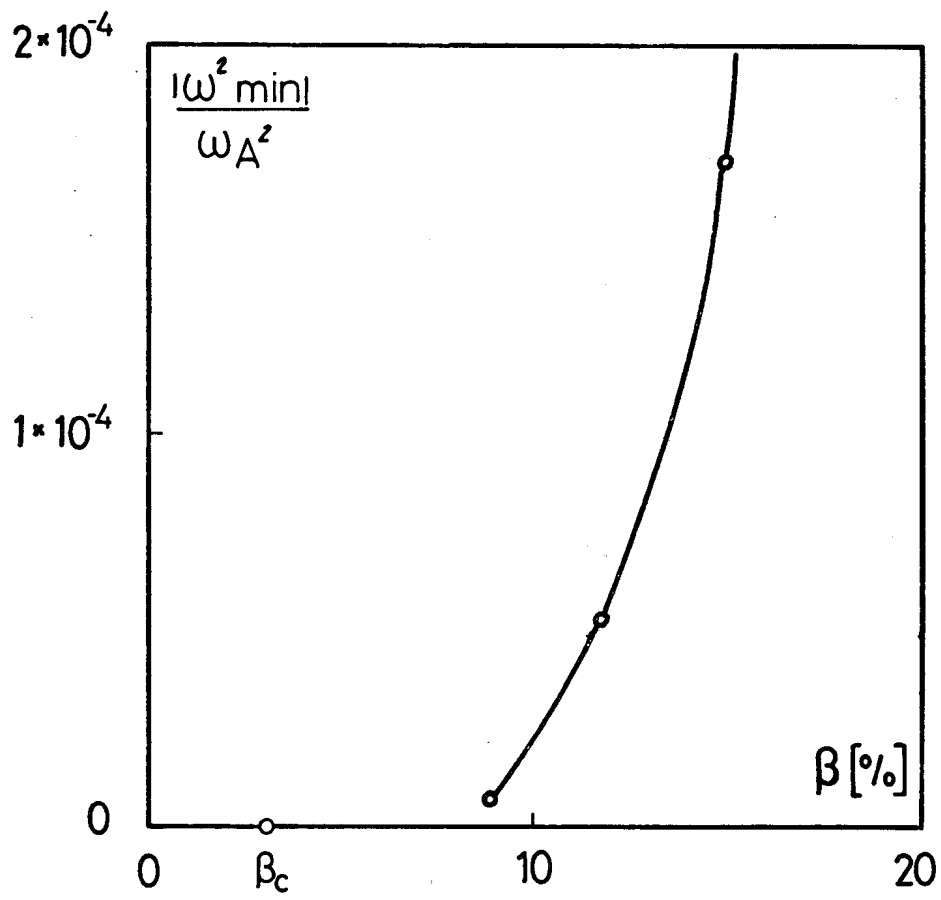
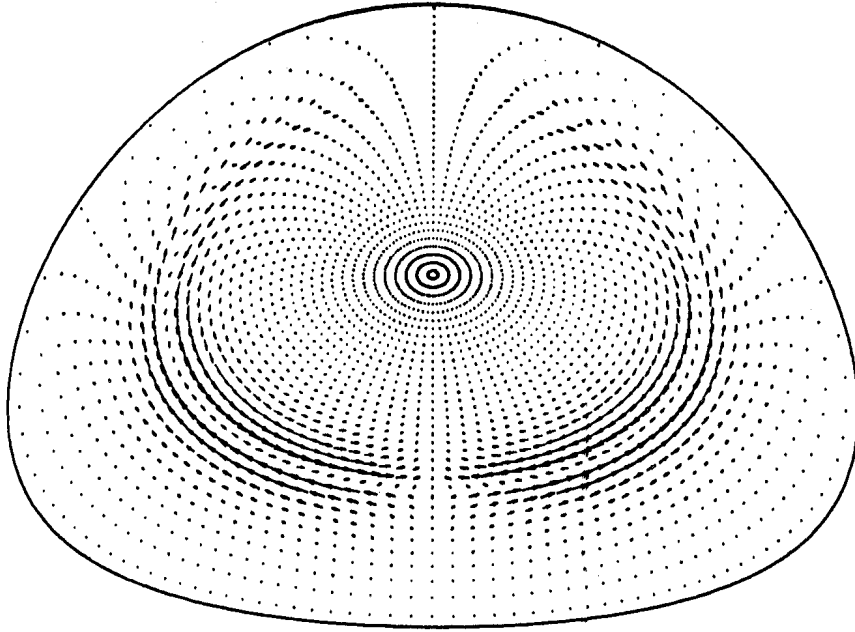
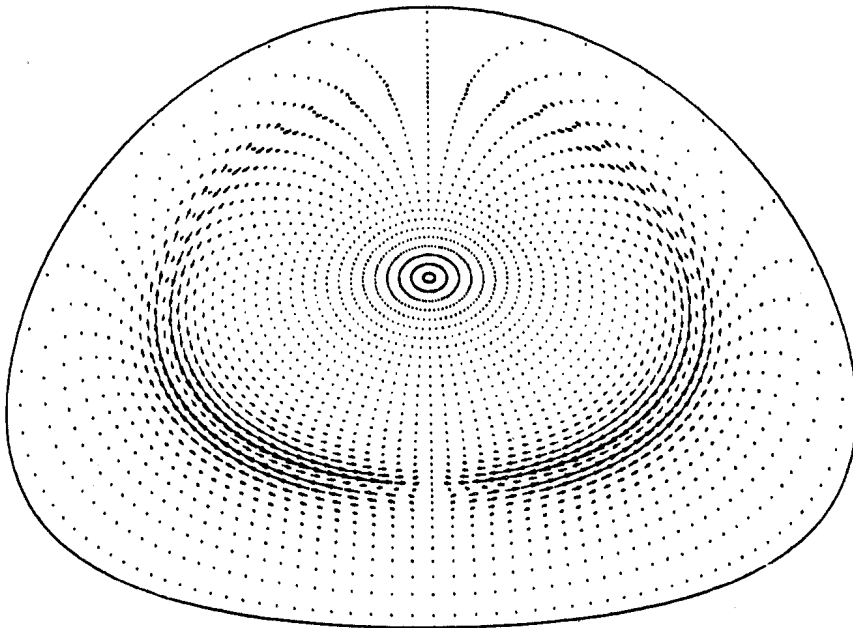


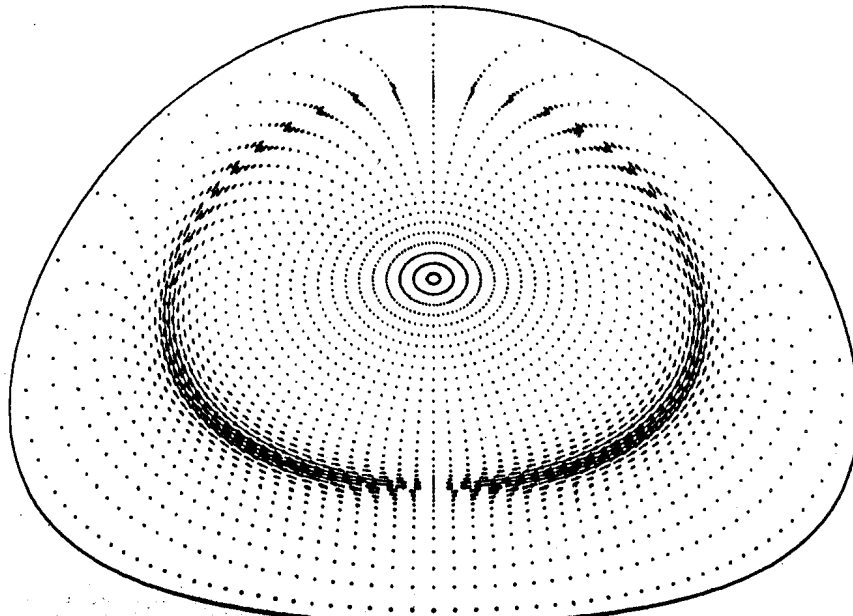
Fig. 6



$\beta = 14,9\%$



$\beta = 11,8\%$



$\beta = 8,8\%$

Fig. 7

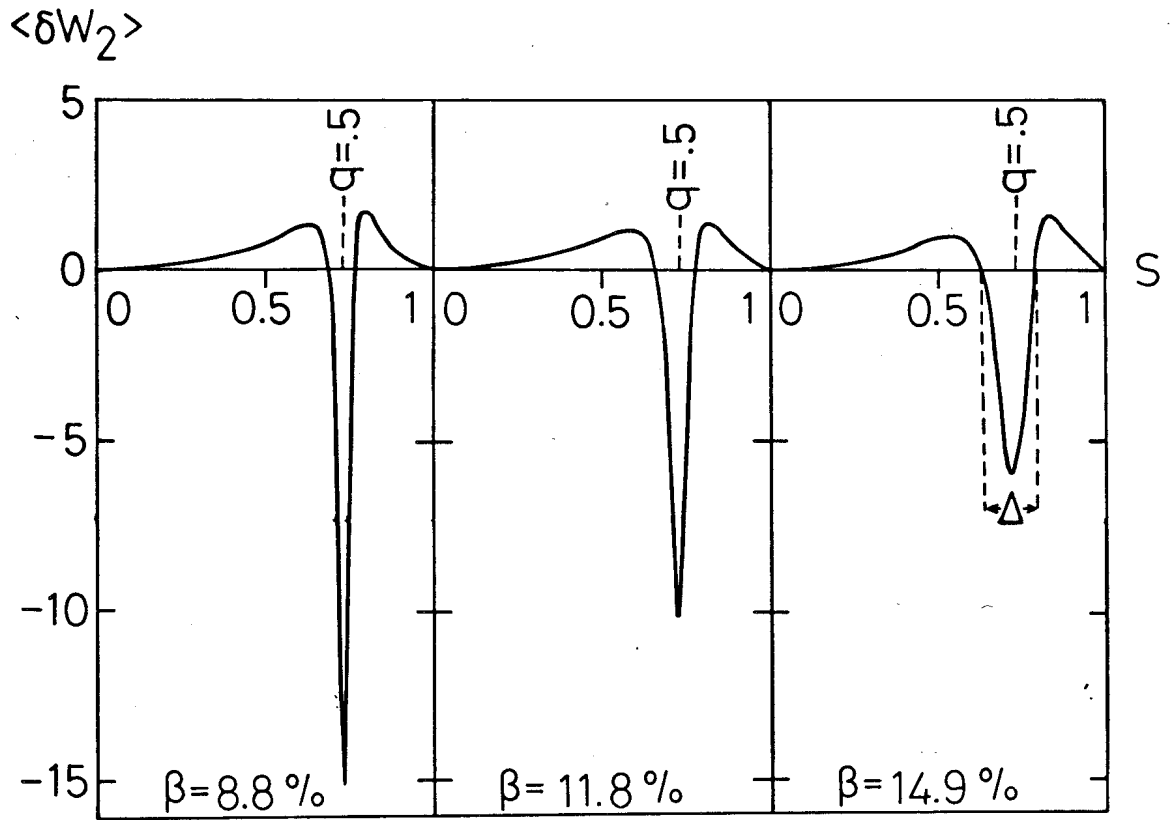


Fig. 8

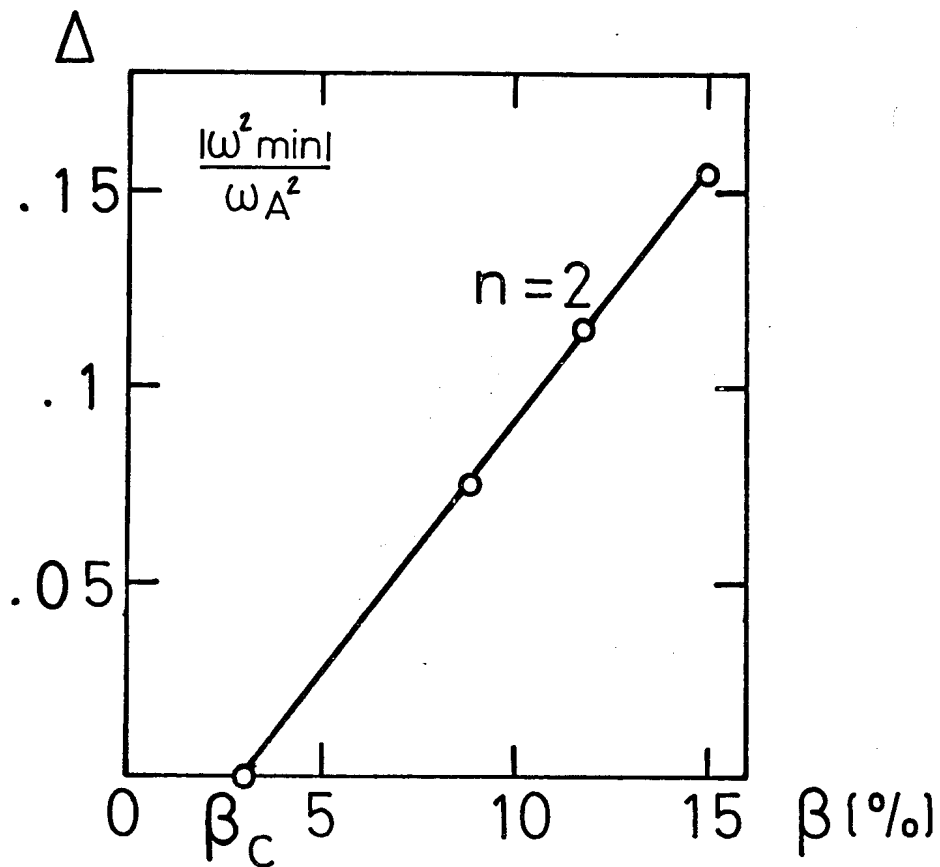


Fig. 9